JOURNAL OF MATERIALS SCIENCE **27** (1992) 3359–3364

Magnetic properties of solid and liquid AuFe alloys

P. TERZIEFF
Institut für Anorganische Chemie der Universität Wien, Währingerstraße 42, A-1090 Wien, Austria

E. WACHTEL
Max-Planck-Institut für Metallforschung, Institut für Werkstoff-wissenschaften, Seestraße 75, D-7000 Stuttgart 1, Germany

The magnetic behaviour of dilute AuFe alloys up to 21 at% Fe was determined by susceptibility measurements between 300 and 1600 K. Judged by the experimentally derived effective magnetic moments and the paramagnetic Curie temperatures, the local environment around the iron atoms in the liquid state is obviously not very different from that in the solid state. The magnetic moments decrease with increasing solute concentration, and the interactions between the solute atoms are indicated to be negative in the dilute alloys and positive in the more concentrated alloys.

1. Introduction

The peculiar magnetic properties of quenched $\underline{\mathrm{Au}}\mathrm{Fe}$ alloys, their extreme sensitivity to the thermal treatment, and the obvious occurrence of clustering effects have been the incentives for a huge number of articles. According to the phase diagram, the extensive solubility of iron in solid gold at high temperatures (74 at % Fe at 1440 K) reduces to less than ≈ 5 at % Fe at room temperature [1]. By quenching, the fcc solid solution can be retained in a supersaturated condition. Thus, it was clear from the outset that the thermodynamic instability of the quenched solid solution at room temperature was one of the most crucial factors.

In some very early papers [2, 3] it had been pointed out that the observed phenomena (such as ageing effects or unexpected magnetization characteristics) are not simply due to the precipitation of iron particles out of the supersaturated fcc solid solution. The inference was that, prior to the expected precipitation of α-Fe particles, the quenched solid solution passes through some transient, but still homogeneous, pre-stage.

In view of the close correlation between the magnetic behaviour of the solute atoms and their local environment, it is not surprising that much attention has been paid to magnetic measurements; however, most of the measurements refer to quenched samples and their low-temperature behaviour. For the reactions in homogeneous phase and the precipitation process itself, the evidence provided by other techniques is even more informative.

Despite the huge number of investigations in this field, attempts to identify the observed phenomena yielded, in many respects, controversal views. Based on diffuse X-ray scattering, Dartygе *et al.* [4] suggested the segregation of iron atoms into small plate-like regions (Guinier–Preston zones), an interpretation meanwhile confirmed by Marsh *et al.* [5], Ju *et al.* [6], and the most recent transmission electron microscopy work of Chen-Chia Chou *et al.* [7].

However, according to the Mössbauer spectroscopy measurements reported by Yoshida *et al.* [8], $\underline{\mathrm{Au}}\mathrm{Fe}$ tends rather to a short-range order of unlike atoms than to a clustering of like atoms. The most recent Mössbauer spectroscopy study combined with X-ray diffraction and small-angle scattering definitely fails to provide evidence for the formation of homogeneously distributed iron clusters [9]. Magnetically, $\underline{\mathrm{Au}}\mathrm{Fe}$ is one of the classical spin glass systems, and therefore efforts have been devoted to elaborate the borderlines between the paramagnetic, the ferromagnetic and the spin-glass state. In the classification of some magnetic transformations, some controversies still remain [10, 11], and the tentative magnetic phase diagram discussed in the literature reflects the complexity of the system [12–16].

The present work was never focused on this very interesting low-temperature behaviour, neither was it aimed at studying the disputed segregation effect in detail. However, it was of particular interest to find out whether the tendency towards clustering or ordering is somehow reflected in the liquid state. The supplementary measurements on solid alloys were included so as to have a reliable reference and to understand better the systematic changes from the solid to the liquid state.

2. Experimental procedure

Samples with a total mass of ≈ 0.5 g were synthesized by directly alloying appropriate amounts of the pure elements. Gold sheet with a nominal purity of 99.99%

and iron wire with a purity of 99.998% were applied as starting materials. The mixtures were sealed under vacuum (quartz, ≈ 0.01 Pa) and thermally treated at 1400 K for 15 h so as to achieve the homogenization of the melts. In order to keep the thermal treatment identical to that during the magnetic measurements, the samples were cooled to room temperature at a rate of 5 K min^{-1}. The magnetic susceptibilities were recorded on a Faraday-type balance, generally at the maximum field strength of 1.38×10^6 A m^{-1}. In order to elaborate the field strength dependence, the magnetic field was varied stepwise between 0.52 and 1.38 $\times 10^6$ A m^{-1}. The temperature, programmable up to 1600 K, was controlled with a Pt–Pt/Rh thermocouple. Except for some very particular cases, the heating and cooling rate was 5 K min^{-1}. The immense number of data points (up to about 2000 points per alloy taken at a variable scanning rate of 1–6 points/min) was represented by smooth curves. The scattering of the data including all the systematic errors was much better than 1×10^{-11} $\text{m}^3 \text{mol}^{-1}$.

During measurements the alloys were kept in open alumina crucibles, protected against oxidation by a continually recycled argon atmosphere. The contributions of the thermocouple and the individual alumina containers were determined by separate measurements. On an absolute scale, the reported magnetic susceptibilities were estimated to be accurate within about 3%.

3. Results and discussion

In order to cover both the dilute and the more concentrated range of <u>Au</u>Fe alloys with the nominal compositions of 1, 3, 6, 9, 12, 15, 18, and 21 at % Fe were subjected to magnetic measurements. The results are summarized in Figs 1 and 2. As a general feature, the discontinuities around 1330 K are due to the solid–liquid transition in accordance with the phase diagram [1]. It is evident that throughout the range of compositions the magnetic character of the system seems to be determined by the solute. Even small additions of iron (1 at % Fe, 3 at % Fe) are effective in transforming the diamagnetism of the host metal into a highly temperature dependent paramagnetism (Fig. 1). This is certainly the consequence of the magnetic moments introduced via the solute atoms; however, for the dilute case the relation between the inverse experimental susceptibility, (χ_m^{-1}), and the temperature, T, is non-linear.

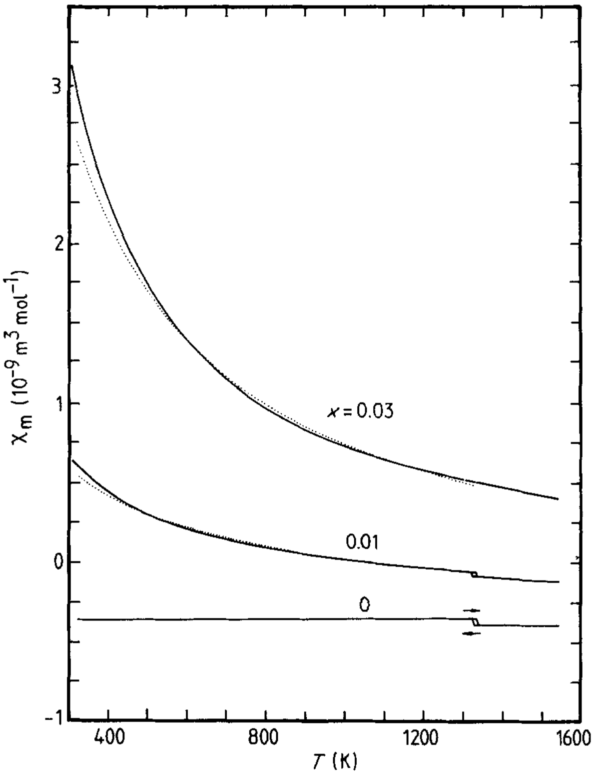

Figure 1 Magnetic susceptibility of solid and liquid dilute $\text{Au}_{1-x}\text{Fe}_x$ alloys as function of temperature: (—) experimental, (· · ·) fitted by Equation 1.

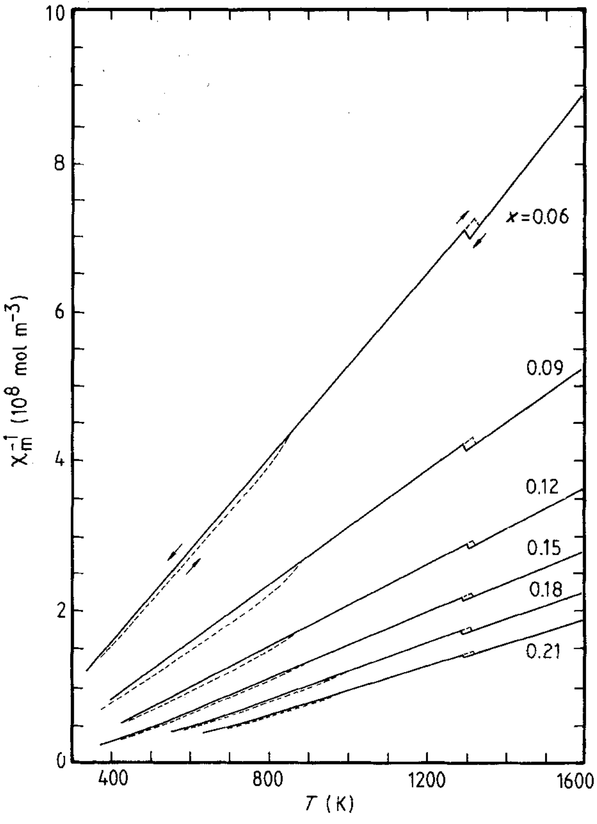

Figure 2 Inverse magnetic susceptibility of solid and liquid $\text{Au}_{1-x}\text{Fe}_x$ alloys as function of temperature: (– –) heating, (——) cooling.

Emphasizing only the cooling curves, those alloys with iron concentrations of more than ≈ 5 at % Fe exhibit a linear relationship between χ_m^{-1} and T, both in the solid as well as in the liquid state (Fig. 2). The departures from the strict linearity observed below 500–700 K in the more concentrated alloys (15, 18, and 21 at % Fe) and the pronounced divergences between the initial heating and the subsequent cooling curves, are doubtlessly due to the instability of the supersaturated solid solution [1]. Because the thereby induced redistribution effect progresses even at room temperature [3], it was expected to find that the samples aged at ambient temperature for more than 3 weeks (i.e. the time interval between preparation and measurement) were in a different condition from those obtained immediately from the melt after solidification. Without specifying the type of solid state reaction which might have occurred (atomic short-range order, clustering, or precipitation of small iron particles) we ascribed the increase in the magnetic susceptibility of the aged alloys to the appearance of a ferromagnetic component. To substantiate this, we attempted to separate the ferromagnetic contribution introduced via the ageing effect by determining the field strength dependence of the magnetic susceptibility. As an example, the alloy with 9 at % Fe was subjected to different thermal treatments achieved by cooling the homogenized melt at different rates (2, 5 and 10 K min^{-1}) from 1450 K down to room temperature. Because, prior to the measurements, the samples were kept at room temperature for some time (12–24 h), the thermal treatment was not well defined but distinctly different due to the different cooling rates. In fact, it became apparent that low cooling rates favour the redistribution process as indicated by the increased susceptibility and its augmented dependence on the magnetic field (Fig. 3). As the magnetic field approaches infinity (i.e. $H^{-1} \rightarrow 0$) the magnetic susceptibilitites tend, in a non-linear, way to some lower value which represents the extrapolated susceptibility of the matrix. Fitting the experimental points with a polynomial up to the second order of H^{-1}, yields $(1.03 \pm 0.17) \times 10^{-2}$ J T^{-1} kg^{-1} for the saturation magnetization of the ferromagnetic component and $(1.60 \pm 0.03) \times 10^{-8}$ m^3 mol^{-1} for the susceptibility of the matrix. This compares well with the value of the practically non-aged sample as obtained directly from the melt. The extrapolation of the incomplete cooling curve of Fig. 2 down to room temperature gives $(1.66 \pm 0.03) \times 10^{-8}$ m^3 mol^{-1} which is indeed very close to the matrix value deduced from the aged specimen.

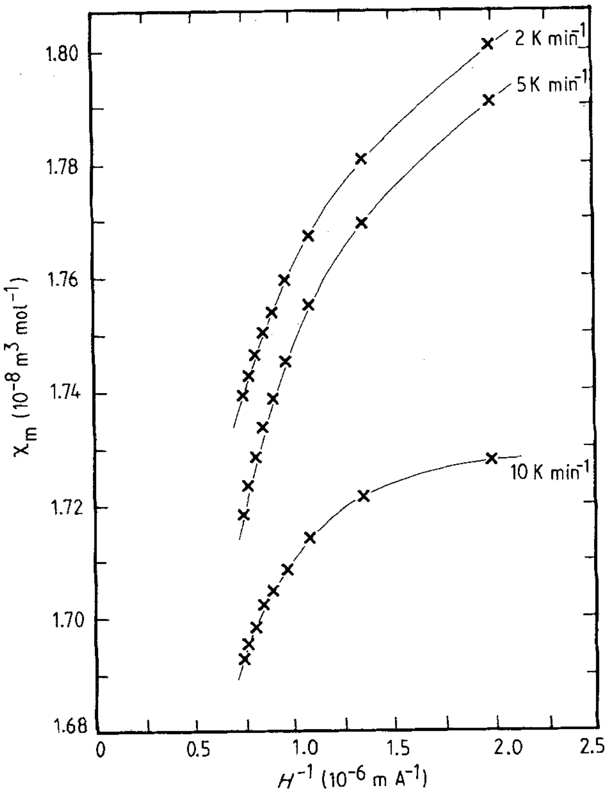

Figure 3 Room-temperature magnetic susceptibility of slowly cooled AuFe (9 at % Fe, 1450 K) as function of the inverse magnetic field.

Based on our magnetic measurements, we may conclude that the solid solution is retained as homogeneous phase as long as the cooling rate is high enough. Nevertheless, for the further treatment of our data we will rely upon the temperature range where the solid solution is, in fact, thermodynamically stable, because we cannot exclude that the debated solid state reactions had already set in during the cooling period. Furthermore, it was interesting to observe that even the dilute alloys with 3 and 6 at % Fe, measured 1 year after their preparation, showed all the characteristics of the ageing process (Fig. 4). However, in view of the extremely long exposure to air, the possible oxidation of the samples in this particular case cannot be excluded.

At this point of the discussion we concede that to some extent our ageing experiments were superficial, but we may also claim that a more profound investigation of this very complex matter certainly goes beyond the scope of this paper.

The quantitative treatment of the experimental data was based on the Curie–Weiss law which predicts a linear variation of χ_m^{-1} with the temperature, T. Although in the concentrated alloys the relationship between χ_m^{-1} and T seemed to be linear over a wide range of temperatures, the correction for the diamagnetic solvent turned out to be indispensable for the dilute alloys. Splitting the total magnetic susceptibility of the alloys, χ_m, into the diamagnetic contribution of the solvent, χ_{Au} and the paramagnetic Curie–Weiss like contribution of the solute we obtain

$$\chi_m = (1 - x_{Fe})\chi_{Au} + \chi_{Fe}\left(\frac{C}{T - \theta_p}\right) \qquad (1)$$

x_{Fe} is the mole fraction of iron, C the Curie constant, and θ_p the paramagnetic Curie temperature; the magnetic moments per iron atom, μ_{eff}, are determined

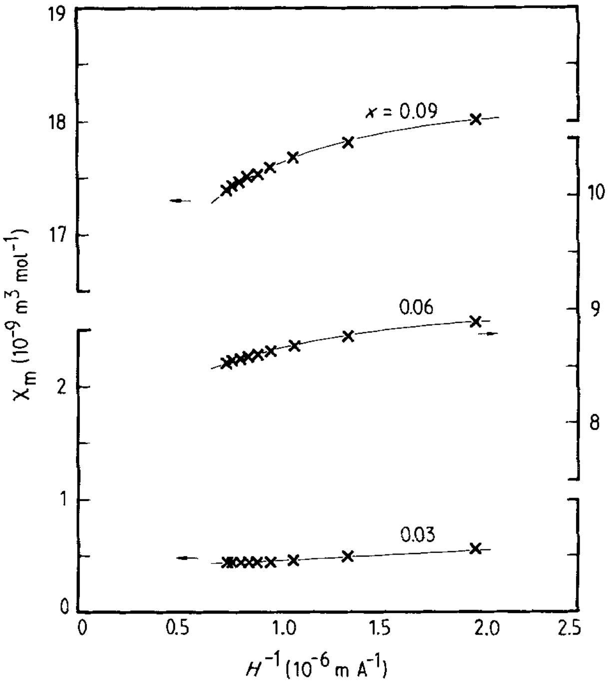

Figure 4 Room-temperature magnetic susceptibility of some dilute $Au_{1-x}Fe_x$ alloys as function of the inverse magnetic field (cooled from 1450 K at 5 K min^{-1}).

from the expression 2.84 $(x_{Fe} \cdot C)^{1/2} \mu_B$. The magnetic susceptibility of solid gold was taken as $(-38.00 + 1.988 \times 10^{-3} T)\ 10^{-11}\ m^3 mol^{-1}$ [17]. The numerical results of the fitting procedure (μ_{eff} and θ_p) are listed in Table I and plotted in Fig. 5, together with the values obtained for the liquid state. Inasmuch as significance is concerned, it must be noted that the outcome of such a treatment is always sensitive to the type of correction, especially in the case of the dilute alloys where the total susceptibilities are relatively small. The estimated errors given in Table I take account of this uncertainty.

Using this modified version, even the dilute alloys with 1 and 3 at % Fe were consistent with the Curie–Weiss law. Fig. 1 compares the experimental curves with those calculated with the help of the parameters given in Table I. In view of the approximate character of the treatment (the assumed additivity of the different contributions to the magnetic susceptibility is only a first approximation), the correlation is acceptable. Moreover, it should be emphasized that for the dilute alloys the subtraction of the matrix susceptibility is more than only a small correction. In the concentrated alloys the fitted curves coincide practically with the experimental curves, consequently they have not been included in Fig. 2.

TABLE I Magnetic moments, (μ_{eff}), and paramagnetic Curie temperatures, (θ_p), of liquid and solid $Au_{1-x}Fe_x$ alloys

Composition x_{Fe}	Magnetic moment, μ_{eff} (μ_B)		Paramagnetic Curie temperature, θ_p (K)	
	Solid	Liquid	Solid	Liquid
0.01	5.14 ± 0.25	5.69 ± 0.62	−139 ± 30	−447 ± 92
0.03	4.94 ± 0.34	5.43 ± 0.25	−58 ± 32	−251 ± 37
0.06	4.76 ± 0.24	5.12 ± 0.20	32 ± 29	−89 ± 29
0.09	4.69 ± 0.14	5.09 ± 0.17	106 ± 19	−49 ± 25
0.12	4.66 ± 0.11	4.92 ± 0.17	180 ± 16	99 ± 25
0.15	4.62 ± 0.11	4.79 ± 0.17	230 ± 16	186 ± 25
0.18	4.54 ± 0.09	4.70 ± 0.17	297 ± 14	253 ± 25
0.21	4.47 ± 0.09	4.60 ± 0.18	361 ± 14	323 ± 26

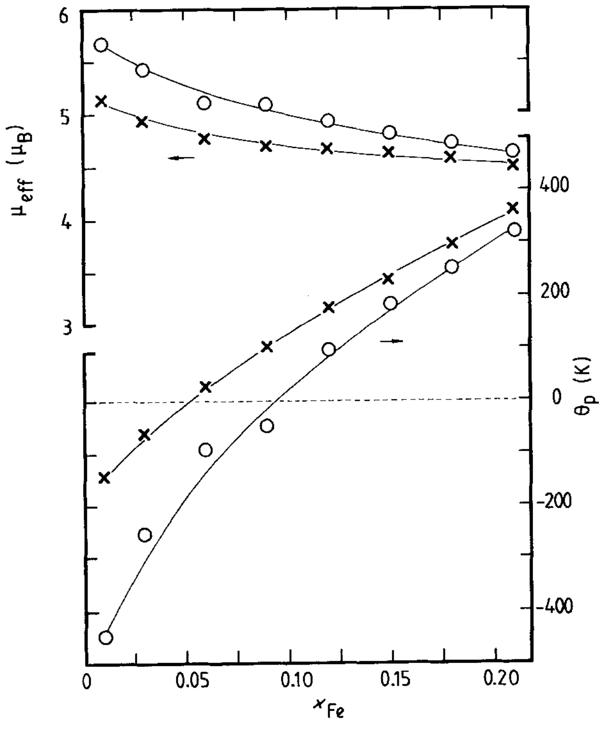

Figure 5 Magnetic moments and paramagnetic Curie temperatures (μ_{eff}, θ_p) of (×) solid and (○) liquid $Au_{1-x}Fe_x$ alloys as function of composition.

The complex magnetic behaviour at low temperatures [12–16] and the pronounced temperature dependence of the magnetic susceptibility have already indicated that the iron atoms are associated with high magnetic moments. In fact, the evaluation yielded values not far from the value expected for a high spin d^6 configuration (4.90 μ_B): 5.14 μ_B for 1 at % Fe and 4.47 μ_B for the alloy with 21 at % Fe.

According to Anderson [18] the magnetic state of a dilute transition metal atom in a non-magnetic matrix is determined by the Coulomb intergral, U, the width of the localized d-level, Δ, and the relative position of the latter with respect to the Fermi level. Large values of U/Δ imply well-separated spin-up and spin-down levels and high magnetic moments, whereas small values of U/Δ represent the non-magnetic case associated with highly overlapping sub-bands. Applied to the case of $\underline{Au}$Fe, we may assume a large Coulomb integral and narrow well-localized d-levels. Within this context we cannot distinguish between well-separated sub-bands with six electrons per iron atom or partially overlapping sub-bands containing five electrons per atom. The magnetic moments of the dilute alloys seem to favour a d^5-configuration because they exceed the value of 4.90 μ_B; however, the differences are still within the limits of our accuracy.

The systematic change of the magnetic moments with the composition suggests a tendency towards a decreasing Coulomb integral and/or an increasing width of the d-states, possibly modified by a systematic change of their position relative to the Fermi level. One of the authors has applied this model in a more quantitative form to the liquid systems Al–Cu–Fe and Al–Cu–Co [19, 20] using the modified and more realistic version put forward by Yosida *et al.* [21]. However, for the tentative interpretation attempted in this paper, the model in its original form was adopted.

As indicated by the sign of the paramagnetic Curie temperatures (Fig. 5) the magnetic interactions are obviously antiferromagnetic up to 5 at % Fe and increasingly ferromagnetic at higher iron contents. It is interesting to find this tendency to some extent also reflected by the low-temperature behaviour of the system. Whereas long-range ferromagnetism dominates the iron-rich side of the solid solution, spin glass behaviour prevails in the dilute region due to the presence of competing antiferromagnetic interactions [12–16].

As far as the agreement with earlier results is concerned, both the magnetic moments and the paramagnetic Curie temperatures compare well with those reported in the literature [2, 3]. Some of the differences, especially those referring to small concentrations of iron, are due to differences in the method of evaluation.

Magnetically, the behaviour of liquid AuFe was found to be not very different from that observed in the solid state. The variation of the magnetic susceptibilities in the range of the liquid and the discontinuities across the solid–liquid transition are shown in Fig. 6. In order to keep the graph on a common scale, the individual curves were shifted systematically downwards by amounts proportional to the iron content of the alloys $(-1.68x_{\mathrm{Fe}} \times 10^{-8}\,\mathrm{m^3\,mol^{-1}})$.

Except for the alloy with 3 at % Fe, the discontinuities caused by the transition from liquid to solid are well pronounced and the transition temperatures are in accordance with the phase diagram [1]. It is remarkable that they change sign with increasing iron content; at the critical concentration of 3 at % Fe the solid transforms into the liquid without any discontinuity. This seems to be incompatible with the melting point discontinuity of pure iron, where the magnetic susceptibility decreases on melting. However, pure liquid iron transforms into a b c c solid whereas in our particular case the melt solidifies as an f c c solid solution; and in fact, it is well known that if supercooled iron crystallizes in the f c c structure the change of the magnetic susceptibility occurs in the opposite direction [22].

Fig. 7 illustrates the composition dependence of the measured magnetic susceptibility and the slope of the uncorrected χ_m^{-1} versus T curves for two representative temperatures. Similar to the features of the solid state, the magnetic susceptibility changes sign around 1 at % Fe and the χ_m^{-1} versus T curves are non-linear below about 5 at % Fe. The increase of χ_m with the concentration is much steeper than predicted by a linear mixing rule but still less pronounced than reported by Güntherodt and Meier [23]. Although the temperature coefficients follow the same trend with the composition, they differ considerably in magnitude. Apart from this numerical disagreement, the slightly convex form of our χ_m versus χ_{Fe} curves matches well the systematic changes through the series Ge–Fe → Ga–Fe → Zn–Fe → Au–Fe.

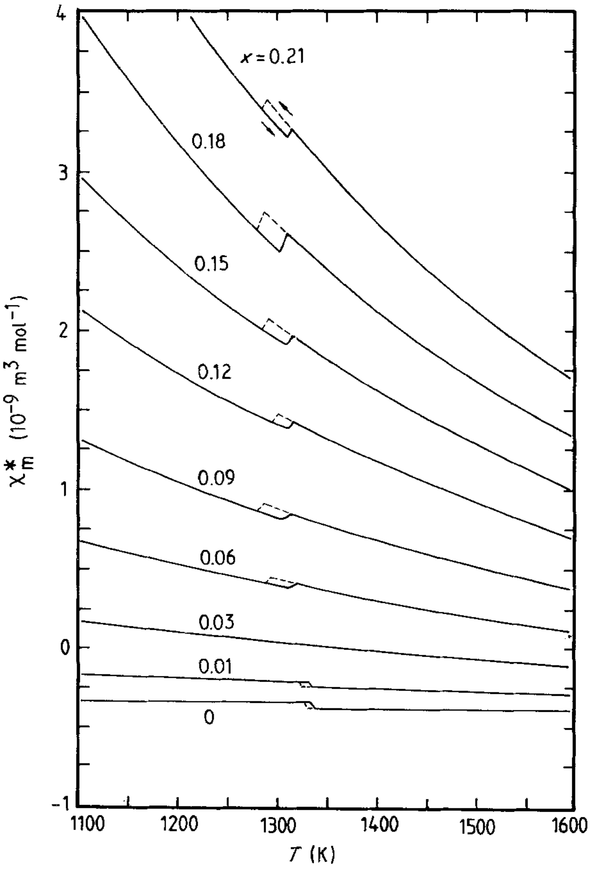

Figure 6 Magnetic susceptibility of liquid $\mathrm{Au_{1-x}Fe_x}$ alloys as function of temperature: (—) heating, (---) cooling. The individual curves are shifted systematically by $-1.68x_{\mathrm{Fe}} \times 10^{-8}\,\mathrm{m^3\,mol^{-1}}$.

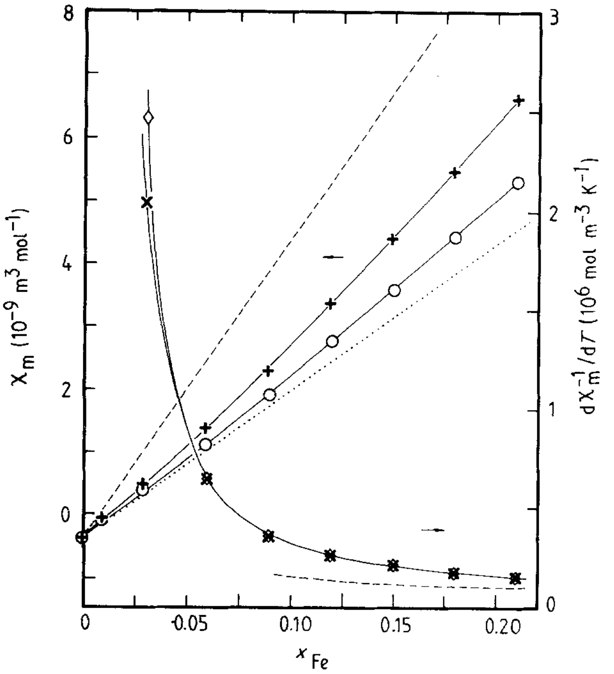

Figure 7 Magnetic susceptibility of liquid $\mathrm{Au_{1-x}Fe_x}$ alloys and the temperature coefficient of χ_m^{-1} as function of composition: (+ , ×) 1340 K; (o, ◇) 1580 K; (---) 1470 K [23]; (···) 1460 K, additive law.

The correction for the liquid-gold matrix was effected with $(-37.74 - 9.42 \times 10^{-4}T) \times 10^{-11}\,\mathrm{m^3\,mol^{-1}}$ [17]. All in all, the experimental data were found to be well represented by Equation 1. Similar to the solid alloys, some divergencies were observed in the case of the dilute alloys; however, they were only small and therefore not shown in Fig. 6. In a previous paper it has been stressed that the magnetic susceptibility of liquid gold is not strictly linear with temperature [17]. The relation given above is only a reasonable approximation and introduces thus an additional uncertainty. The magnitudes of the magnetic moments, μ_{eff}, and the paramagnetic Curie temperatures, θ_p, as well as their variations with the composition of the liquid alloys, are roughly comparable to those of the solid state (Fig. 5). This may be taken as an indication of a similar local environment around the iron atoms in both states. The differences in the absolute values of μ_{eff} and θ_p are only small. Throughout the range of composition the magnetic moments of the liquid are somewhat higher and, conversely, the paramagnetic Curie temperatures are smaller. Accordingly the change in sign of θ_p occurs at a higher iron concentration (9 at % Fe).

At infinite dilution, the magnetic moments seem to approach 5.9 μ_B, the highest possible value for a d^5-configuration. In terms of the Anderson model this implies an even increased U/Δ in the liquid state and/or a changed position of the impurity states relative to the Fermi level. It is difficult to specify this in detail, but the input data of the model are lacking. Likewise increased magnetic moments, although less pronounced, seem to be indicated for manganese, iron and cobalt impurities in liquid copper [24].

We are not surprised to find nothing pointing to a tendency of segregation or short range order in the liquid state. The positive enthalpies of mixing indeed hint at the demixing behaviour of the system [25], while the magnetic properties are primarily dominated by the effect of introducing highly magnetic atoms into a diamagnetic liquid. Although known for quite some time, the appearance of such high magnetic moments in the liquid is once more remarkable. Regardless of the model chosen to explain the magnetic properties, one may safely guess that at least the electronic environment, if not the local environment, is about the same in the liquid and solid state.

Acknowledgement

The authors thank Professor K. L. Komarek for his permanent interest and for critical comments to this article.

References

1. T. B. MASSALSKI, "Binary Alloy Phase Diagrams" (American Society of Metals, Metal Park, OH, 1986).
2. A. R. KAUFMANN, S. T. PAN and J. R. CLARK, *Rev. Mod. Phys.* **17** (1945) 87.
3. E. SCHEIL, H. SPECHT and E. WACHTEL, *Z. Metallkde* **49** (1958) 590.
4. E. DARTYGE, H. BOUCHIAT and P. MONOD, *Phys. Rev. B* **25** (1982) 6995.
5. C. MARSH, S. POLAT and HAYDN CHEN, *Scripta Metall.* **21** (1987) 619.
6. C. P. JU, C. M. WAYMAN and HAYDN CHEN, *ibid.* **21** (1987) 59.
7. CHEN-CHIA CHOU, HAYDN CHEN and C. M. WAYMAN, *Mater. Sci. Engng A* **123** (1990) 21.
8. Y. YOSHIDA, F. LANGMAYR, P. FRATZL and G. VOGL, *Phys. Rev. B* **39** (1989) 6395.
9. P. FRATZL, F. LANGMAYR and Y. YOSHIDA, *ibid.* **44** (1991) 4192.
10. D. BOUMAZOUZA, P. MANGIN, B. GEORGE, P. LOUIS, R. A. BRAND, J. J. RHYNE and R. W. ERWIN, *ibid.* **39** (1989) 749.
11. P. A. BECK, *ibid.* **39** (1989) 752.
12. U. GONSER, R. W. GRANT, C. J. MEECHAN, A. H. MUIR and H. WIEDERSICH, *J. Appl. Phys.* **36** (1965) 2124.
13. V. CANELLA and J. A. MYDOSH, *Phys. Rev. B* **6** (1972) 4220.
14. A. P. MURANI, S. ROTH, P. RADHAKRISHNA, B. D. RAINFORD, B. R. COLES, K. IBEL, G. GOELTZ and F. MEZEI, *J. Phys. F Metal Phys.* **6** (1976) 425.
15. B. R. COLES, B. V. B. SARKISSIAN and R. H. TAYLOR, *Phil. Mag. B* **37** (1978) 489.
16. B. V. B. SARKISSIAN, *J. Phys. F Metal Phys.* **11** (1981) 2191.
17. P. TERZIEFF, K. L. KOMAREK and E. WACHTEL, *ibid.* **16** (1986) 1071.
18. P. W. ANDERSON, *Phys. Rev.* **124** (1961) 41.
19. A. PANTASIS and E. WACHTEL, *J. Mag. Mag. Mater.* **9** (1978) 264.
20. E. BAYER and E. WACHTEL, *Z. Metallkde.* **71** (1990) 410.
21. K. YOSIDA, A. OKIJI and S. CHIKAZUMI, *Prog. Theor. Phys.* **33** (1965) 559.
22. Y. NAGAKAWA, *J. Phys. Soc. Jpn* **11** (1956) 855.
23. H. J. GÜNTHERODT and H. A. MEIER, *Phys. Kondens. Mat.* **16** (1973) 25.
24. J. A. GARDNER and C. P. FLYNN, *Phil. Mag.* **15** (1967) 1232.
25. L. TOPOR and O. J. KLEPPA, *Metall. Trans. B* **15** (1984) 573.

Received 6 June
and accepted 22 October 1991